

NASA Technical Memorandum 78575

(NASA-TM-78575) A SIMPLIFIED ROTOR SYSTEM
MATHEMATICAL MODEL FOR PILOTED FLIGHT
DYNAMICS SIMULATION (NASA) 28 P
HC A03/MP A01

N79-23977

CSCL 01C

G3/08

Unclass
22094

A Simplified Rotor System Mathematical Model for Piloted Flight Dynamics Simulation

Robert T. N. Chen

May 1979



NASA

National Aeronautics and
Space Administration

NASA Technical Memorandum 78575

A Simplified Rotor System Mathematical Model for Piloted Flight Dynamics Simulation

Robert T. N. Chen, Ames Research Center, Moffett Field, California

NASA

National Aeronautics and
Space Administration

Ames Research Center

Moffett Field, California 94035

NOMENCLATURE

- A_{1c} lateral cyclic pitch measured from hub plane and in "wind-hub" system, rad (or deg)
- A_{1s} lateral cyclic pitch measured from hub plane and in hub-body system, rad (or deg)
- a blade lift-curve slope
- a_1 longitudinal first-harmonic flapping coefficient measured from hub plane and in "wind-hub" system, rad
- a_{1s} longitudinal first-harmonic flapping coefficient measured from hub plane and in hub-body system, rad
- a_0 blade coning angle measured from hub plane, rad
- B_{1c} longitudinal cyclic pitch measured from hub plane and in "wind-hub" system, rad (or deg)
- B_{1s} longitudinal cyclic pitch measured from hub plane and in hub-body system, rad (or deg)
- b_1 lateral first-harmonic flapping coefficient measured from hub plane and in "wind-hub" system, rad
- b_{1s} lateral first-harmonic flapping coefficient measured from hub plane and in hub-body system, rad
- C_H H force coefficient, $C_H = \frac{H_F}{\rho \pi R^2 (\Omega R)^2}$
- C_Q torque coefficient, $C_Q = \frac{Q_F}{\rho \pi R^2 (\Omega R)^2 R}$
- C_T thrust coefficient, $C_T = \frac{T_F}{\rho \pi R^2 (\Omega R)^2}$
- C_Y Y force coefficient, $C_Y = \frac{Y_F}{\rho \pi R^2 (\Omega R)^2}$
- c blade chord, m
- e flapping hinge offset, m
- H_F component of main rotor resultant force in the rotor disc plane in $\psi' = 0$ direction, N
- I_F blade moment of inertia about flapping hinge, kg-m^2

- i_F shaft tilt w.r.t. fuselage, positive forward, deg
 K_1 pitch-flap coupling ratio, $\tan \delta_3$
 K_β flapping hinge restraint, N-m/rad
 k_1 desired longitudinal control sensitivity, $k_1 = \frac{\partial a_{1s}}{\partial \delta_L}$
 k_2 desired lateral control sensitivity, $k_2 = \frac{\partial b_{1s}}{\partial \delta_A}$
 L_F main rotor contribution to aircraft rolling moment about body axis x ,
N-m
 L_H rolling hub moment in hub-body system
 L_{HF} main rotor hub moment about x'_s axis, N-m
 M_F main rotor contribution to aircraft pitching moment about body axis y ,
N-m
 M_H pitching hub moment in hub-body system
 M_{HF} main rotor hub moment about y'_s axis, N-m
 M_β blade mass moment about the flapping hinge, kg-m
 N number of blades
 N_F main rotor contribution to aircraft yawing moment about body axis z ,
N-m
 P ratio of flapping frequency to rotor system angular velocity
 p aircraft roll rate, rad/sec
 p_w aircraft roll rate in wind-hub system, rad/sec, $p_w = p \cos \beta_w + q \sin \beta_w$
 \dot{p} aircraft roll acceleration, rad/sec²
 Q_F main rotor torque about z'_s axis, N-m
 q aircraft pitch rate, rad/sec
 q_w aircraft pitch rate in wind-hub system, rad/sec, $q_w = -p \sin \beta_w + q \cos \beta_w$
 \dot{q} aircraft pitch acceleration, rad/sec²
 R rotor radius, m

- r aircraft yaw rate, rad/sec
 r' radial station of the blade element measured from the flapping hinge, m
 T_F main rotor thrust force acting perpendicular to rotor disc plane, N
 V true airspeed, m/sec
 v_i uniform induced velocity, $v_i = \frac{C_T(\Omega R)}{2(\mu^2 + \lambda^2)^{1/2}}$, m/sec
 X_F main rotor force along body axis, x, N
 x nondimensional radial station of the blade element, $x = \frac{e + r'}{R}$
 x_s }
 y_s } wind-hub system
 z_s }
 x'_s }
 y'_s } hub-body system
 z'_s }
 Y_F component of main rotor resultant force in the rotor disc plane in $\psi' = 90^\circ$ direction, N
 Z_F main rotor force along body axis z, N
 α hub plane angle of attack, deg
 β blade flapping angle measured from hub plane, rad (or deg)
 β_w rotor sideslip angle, that is, the angle between x_s and x'_s , deg
 γ Lock number, $\frac{\rho a c R^4}{I_\beta}$
 δ blade mean profile drag coefficient
 δ_A lateral control displacement
 δ_L longitudinal control displacement
 ϵ e/R
 θ blade pitch angle measured from hub plane,
 $\theta = \theta_0 - A_{1c} \cos \psi - \beta_{1c} \sin \psi + x\theta_t - K_1\beta$, rad (or deg)

- θ_0 blade-root collective pitch measured from hub plane, rad
 θ_t total blade twist (tip with respect to root), deg
 λ inflow ratio, $\frac{V \sin \alpha - v_1}{\Omega R}$
 μ advance ratio, $\frac{V \cos \alpha}{\Omega R}$
 ρ air density, kg/m³
 σ rotor solidity ratio
 ϕ control advance angle
 ψ azimuth angle measured from downwind in the sense of rotor rotation, rad
 (or deg)
 ψ' azimuth angle measured from $-x'_s$ in the sense of rotor rotation, deg
 Ω rotor system angular velocity, rad/sec

A SIMPLIFIED ROTOR SYSTEM MATHEMATICAL MODEL FOR
PILOTED FLIGHT DYNAMICS SIMULATION

Robert T. N. Chen

Ames Research Center

SUMMARY

This report documents a simplified analytical mathematical model of the helicopter main rotor; the model was developed primarily for real-time pilot-in-the-loop investigation of helicopter flying qualities. The mathematical model explicitly includes the tip-path plane dynamics and several primary rotor design parameters, such as flapping hinge restraint, flapping hinge offset, blade Lock number, and pitch-flap coupling. The model has been used in several exploratory studies, recently performed at Ames Research Center, of the flying qualities of helicopters with a variety of rotor systems.

The report describes the basic assumptions used and the major steps involved in the development of the set of equations listed. The equations consist of the tip-path plane dynamic equation, the equations for the main rotor forces and moments, and the equation for control phasing required to achieve decoupling in pitch and roll due to cyclic inputs.

INTRODUCTION

There is a need for an expanded flying-qualities data base for use in developing design criteria for future helicopters. A safe and cost effective way to establish such a data base is to conduct exploratory investigations, using piloted ground simulation techniques, and to then substantiate the results in-flight by using variable-stability research helicopters.

Mathematical models for real-time, piloted, ground simulation valid for specific missions and tasks are therefore needed. Unfortunately, several existing general purpose helicopter simulation models, such as the "C-81" (ref. 1) and "REXOR" (ref. 2), are not suitable for real-time applications. These sophisticated blade-element models are far beyond the capability of current-generation computers for real-time simulation. Moreover, because they are aimed at multidisciplinary users, they are inefficient and often do not provide the insight needed for designing experiments for investigating general flying qualities.

Simpler flight dynamic models for piloted simulation exist (refs. 3, 4), but they are for specific existing helicopters. Also, these models are quasi-static in nature and do not explicitly account for the dynamic effect of rotor modes, such as rotor-blade flapping, which can be important in studies of flying qualities. Therefore, there is a need to develop general but simplified

flight dynamic models for exploratory studies of flying qualities and flight-control systems and, especially, for use on ground simulators that have only moderate computational speed and capacity.

This report presents a simplified general main rotor mathematical model that has been used in experimental design analyses and ground-simulator investigations of helicopter flying qualities in visual terrain flying tasks and instrument flight tasks at Ames Research Center (refs. 5-7).¹ The model explicitly contains rotor system design parameters, such as flapping hinge restraint, effective hinge offset, blade Lock number, and pitch-flap coupling, as shown in figure 1. These parameters have been used in appropriate combinations to cover a wide variety of rotor systems.

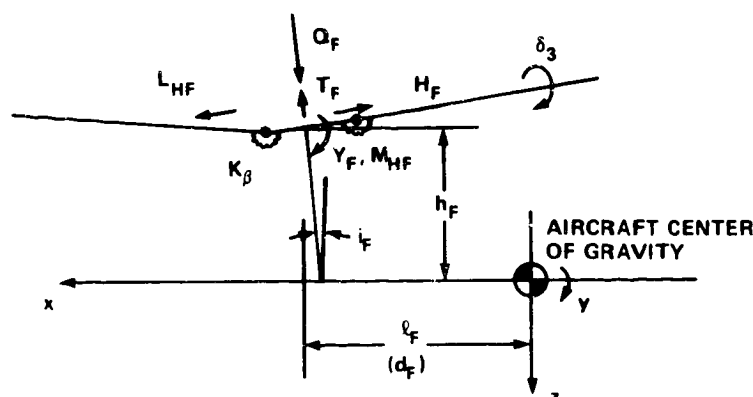


Figure 1.- Main rotor configuration and parameters.

The report also describes the tip-path plane dynamic equation, the development of the main rotor force and moment expressions, and the control-mixing equation for decoupling pitching and rolling moments due to cyclic control displacement in the cockpit.

TIP-PATH-PLANE APPROXIMATION FOR FLAPPING DYNAMICS

Essential to the main rotor mathematical model is the description of the blade-flapping dynamics. For the model described in this report, the flapping dynamics were approximated using a tip-path plane representation. A detailed description of the development was given in reference 8. For present purposes, a brief summary of the basic assumptions used and the major steps involved in the development is presented.

¹Miyajima, K.; and Chen, R. T. N.: Analytical and Experimental Study of an Advanced Stability and Control Augmentation System for a Hingeless Rotor Helicopter (in preparation).

Basic Assumptions

The flapping equation of motion of the rotor blade was first developed using the following assumptions. The assumptions are similar to those used for the "classical" equations (refs. 9 and 10).

1. Rotor blade was rigid in bending and torsion, and the twist of the blade was linear.
2. The flapping angle and inflow angle were assumed to be small and the analysis utilized a simple strip theory.
3. The effects of the aircraft motion on the blade flapping were limited to those due to the angular acceleration \dot{p} and \dot{q} , the angular rate p , q , and the normal acceleration.
4. The reversed flow region was ignored and the compressibility and stall effects disregarded.
5. The inflow was assumed to be uniform and no inflow dynamics were used.
6. The tip loss factor was assumed to be 1.

The flapping equation of motion for a two-bladed teetering rotor and N-bladed nonteetering rotors are given in appendix A. They explicitly contain the primary design parameters, such as flapping hinge restraint, hinge offset, blade Lock number, and pitch-flap coupling. The blade flapping, $\beta(t)$, in those equations was then approximated by the first harmonic terms with time-varying coefficients; that is,

$$7. \quad \beta(t) = a_0(t) - a_1(t)\cos \psi - b_1(t)\sin \psi$$

The first and second time derivatives of $\beta(t)$ are therefore,

$$\dot{\beta}(t) = \dot{a}_0(t) - [\dot{a}_1(t) + b_1(t)\Omega]\cos \psi - [\dot{b}_1(t) - a_1(t)\Omega]\sin \psi$$

$$\ddot{\beta}(t) = \ddot{a}_0 - (\ddot{a}_1 + 2\dot{b}_1\Omega - a_1(-)\cos \psi - (\dot{b}_1 - 2\dot{a}_1\Omega - b_1\Omega^2)\sin \psi$$

Tip-Path Plane Dynamic Equation

For the nonteetering N-bladed rotor, the time-varying coefficients, $a_0(t)$, $a_1(t)$, and $b_1(t)$ are obtained by equating the constant term and the terms with $\sin \psi$ and $\cos \psi$ in the flapping equation (A2) using the above equations. The result is the following set of tip-path plane dynamic equations:

$$\ddot{a} + \dot{D}\dot{a} + \dot{K}a = \dot{\xi}$$

$$\dot{D} = 0 \quad \left[\begin{array}{ccc} \frac{\gamma}{2} \left(\frac{1}{4} - \frac{2}{3} \epsilon + \frac{\epsilon^2}{2} \right) & 0 & -\frac{\gamma\mu}{4} \left(\frac{1}{3} - \epsilon + \epsilon^2 \right) \\ 0 & \frac{\gamma}{2} \left(\frac{1}{4} - \frac{2}{3} \epsilon + \frac{\epsilon^2}{2} \right) & 2 \\ -\frac{\gamma\mu}{2} \left(\frac{1}{3} - \epsilon + \epsilon^2 \right) & -2 & \frac{\gamma}{2} \left(\frac{1}{4} - \frac{2}{3} \epsilon + \frac{\epsilon^2}{2} \right) \end{array} \right]$$

$$K = \mu^2 \quad \left[\begin{array}{ccc} \frac{\gamma K_1 \mu^2}{4} \left(\frac{1}{2} - \epsilon + \frac{\epsilon^2}{2} \right) & -\frac{\gamma\mu}{4} \left(\frac{\epsilon}{2} - \epsilon^2 \right) & -\frac{\gamma K_1 \mu}{4} \left(\frac{2}{3} - \epsilon \right) \\ -\frac{\gamma\mu}{2} \left(\frac{1}{3} - \frac{\epsilon}{2} \right) & p^2 - 1 + \frac{\gamma K_1 \mu^2}{8} \left(\frac{1}{2} - \epsilon + \frac{\epsilon^2}{2} \right) & \frac{\gamma}{2} \left(\frac{1}{4} - \frac{2}{3} \epsilon + \frac{\epsilon^2}{2} \right) + \frac{\gamma\mu^2}{8} \left(\frac{1}{2} - \epsilon + \frac{\epsilon^2}{2} \right) \\ -\frac{\gamma K_1 \mu}{2} \left(\frac{2}{3} - \epsilon \right) & -\frac{\gamma}{2} \left(\frac{1}{4} - \frac{2}{3} \epsilon + \frac{\epsilon^2}{2} \right) + \frac{\gamma\mu^2}{8} \left(\frac{1}{2} - \epsilon + \frac{\epsilon^2}{2} \right) & p^2 - 1 + \frac{3}{8} \gamma K_1 \mu^2 \left(\frac{1}{2} - \epsilon + \frac{\epsilon^2}{2} \right) \end{array} \right]$$

$$f = \Omega^2 \quad \left[\begin{array}{ccc} -\frac{5M}{I_3 \Omega^2} + \frac{\gamma}{2} \left[\left(\frac{1}{4} - \frac{2}{3} \epsilon \right) + \frac{\mu^2}{2} \left(\frac{1}{2} - \epsilon + \frac{\epsilon^2}{2} \right) \right] \theta_0 - \frac{\gamma}{2} \left[\mu \left(\frac{1}{3} - \frac{\epsilon}{2} \right) \right] B_{1c} + \frac{\gamma}{2} \left[\left(\frac{5}{4} - \frac{\epsilon}{2} \right) + \frac{\mu^2}{2} \left(\frac{1}{3} - \frac{\epsilon}{2} \right) \right] \theta_t + \frac{\gamma}{2} \left(\frac{1}{3} - \frac{\epsilon}{2} \right) \lambda \\ + \frac{\gamma}{8} \mu \left(\frac{2}{3} - \epsilon \right) \left(\frac{p}{\Omega} \cos \beta_w + \frac{q}{\Omega} \sin \beta_w \right) \\ -2 \left(1 + \frac{eM_3}{I_3} \right) \left(\frac{p}{\Omega} \cos \beta_w + \frac{q}{\Omega} \sin \beta_w \right) + \left(\frac{p}{\Omega^2} \sin \beta_w - \frac{q}{\Omega^2} \cos \beta_w \right) + \frac{\gamma}{2} \left[\left(\frac{1}{4} - \frac{2}{3} \epsilon \right) + \frac{\mu^2}{4} \left(\frac{1}{2} - \epsilon + \frac{\epsilon^2}{2} \right) \right] A_{1c} \\ + \frac{\gamma}{2} \left(\frac{1}{4} - \frac{2}{3} \epsilon \right) \left(\frac{p}{\Omega} \sin \beta_w - \frac{q}{\Omega} \cos \beta_w \right) \\ -2 \left(1 + \frac{eM_3}{I_3} \right) \left(\frac{p}{\Omega} \sin \beta_w - \frac{q}{\Omega} \cos \beta_w \right) - \left(\frac{p}{\Omega^2} \cos \beta_w + \frac{q}{\Omega^2} \sin \beta_w \right) - \frac{\gamma}{2} \mu \left(\frac{2}{3} - \epsilon \right) \theta_0 - \frac{\gamma\mu}{2} \left(\frac{1}{2} - \frac{2\epsilon}{3} \right) \theta_t \\ + \frac{\gamma}{2} \left[\left(\frac{1}{4} - \frac{2}{3} \epsilon \right) + \frac{3\mu^2}{4} \left(\frac{1}{2} - \epsilon + \frac{\epsilon^2}{2} \right) \right] B_{1c} - \frac{\gamma\mu}{2} \left(\frac{1}{2} - \epsilon + \frac{\epsilon^2}{2} \right) \lambda - \frac{\gamma}{2} \left(\frac{1}{4} - \frac{2}{3} \epsilon \right) \left(\frac{p}{\Omega} \cos \beta_w + \frac{q}{\Omega} \sin \beta_w \right) \end{array} \right]$$

(1)

where

$$p^2 = 1 + \frac{K_\beta}{I_\beta \Omega^2} + \frac{eM_\beta}{I_\beta} + \frac{\gamma K_1}{8} \left(1 - \frac{4}{3} \epsilon\right)$$

and

$$\underline{a} = (a_0, a_1, b_1)^T$$

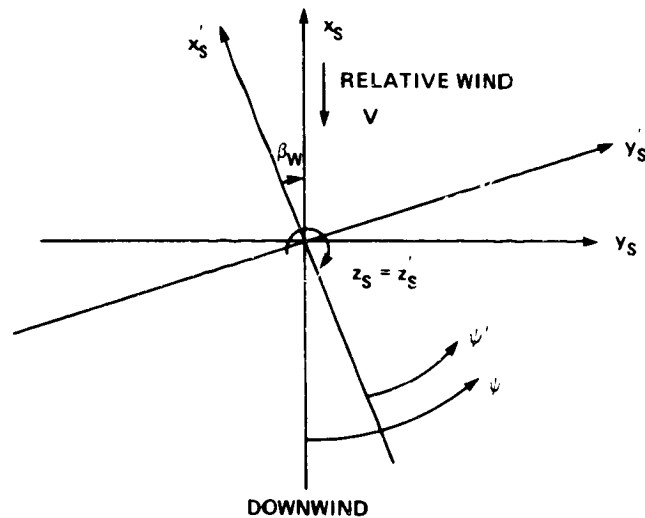
For a two-bladed teetering rotor, the tip-path plane representation loses its physical meaning. However, if the approximation of item (7) above for the blade flapping is employed, then a_0 is to be treated as a preset constant. The coefficients $a_1(t)$ and $b_1(t)$ can then be solved by setting $\epsilon = \dot{a}_0 = \ddot{a}_0 = 0$ in equation (1).

MAIN ROTOR FORCES AND MOMENTS

The main rotor thrust, the H and Y forces, the hub moments, and the torque were developed for the rotor system of interest. In the development of these forces and moments, the same set of basic assumptions (1 through 7, above) discussed in conjunction with the development of the tip-path plane dynamic equations was utilized. Thus, aerodynamically, momentum theory was used in conjunction with the uniform inflow; simple strip theory was utilized and the blade forces were analytically integrated over the radius. Because the reversed flow region and the stall and compressibility effects were ignored, the total rotor forces and moments were again analytically obtained by summing the contributions, to each blade, that were analytical functions of the azimuth. Because of these assumptions and simplifications, the results of the analysis are valid only for a limited range of flight conditions. Nevertheless, a previous study (ref. 10) has shown that this type of analysis is valid for stability and control investigations of the rotorcraft up to an advance ratio of about 0.3. Also, similar to the development of the tip-path plane dynamic equations, these rotor forces and moments were first obtained in the wind-hub coordinate system. They were then transformed into the hub-body system (see fig. 2).

The forces and moments thus developed contain periodic terms; the highest harmonic terms correspond directly to the number of rotor blades. For example, for a three-bladed rotor, the force and moment equations contain only 3/revolution harmonic terms, and for a four-bladed rotor, 4/revolution harmonic terms (this is shown in appendix B).

With the harmonic terms dropped, the force and moment expressions for a nonteetering rotor are as follows.



x_s, y_s, z_s = ROTCR "HUB-BODY" SYSTEM

x_s, y_s, z_s = ROTOR "HUB-WIND" SYSTEM

Figure 2.- Coordinate systems for the main rotor.

Main Rotor Thrust

The main rotor thrust expression for a nonteetering rotor is:

$$\begin{aligned}
 T_F = \frac{N}{2} \rho a c R (\Omega R)^2 & \left\{ \frac{1}{2} (1 - \epsilon^2) \lambda + \theta_0 \left[\frac{1}{3} + \frac{\mu^2}{2} (1 - \epsilon) \right] + \theta_t \left[\frac{1}{4} + \frac{\mu^2}{4} (1 - \epsilon^2) \right] \right. \\
 & - \frac{\mu}{2} (1 - \epsilon^2) (B_{1c} - K_1 b_1) - a_0 \left[\frac{1}{3} + \frac{\mu^2}{2} (1 - \epsilon) \right] K_1 + a_1 \left[\frac{\mu}{2} \epsilon (1 - \epsilon) \right] \\
 & - \frac{\dot{a}_0}{\Omega} \left(\frac{1}{3} - \frac{\epsilon}{2} \right) + \frac{\dot{b}_1}{\Omega} \left[\frac{\mu}{4} (1 - \epsilon)^2 \right] \\
 & \left. + \frac{\mu}{4} (1 - \epsilon^2) \left(\frac{p}{\Omega} \cos \beta_w + \frac{q}{\Omega} \sin \beta_w \right) \right\} - N M_B \ddot{a}_0 \quad (2)
 \end{aligned}$$

Main Rotor H and Y Forces in Hub-Body System

The expressions for the main rotor H and Y forces in the hub-body system are:

$$H_F = \frac{N}{2} \rho a c R (\Omega R)^2 \frac{2C_H}{a\sigma} \quad (3)$$

$$Y_F = \frac{N}{2} \rho a c R (\Omega R)^2 \frac{2C_Y}{a\sigma} \quad (4)$$

where

$$\frac{2C_H}{a\sigma} = \left(\frac{2C_H}{a\sigma}\right)_w \cos \beta_w + \left(\frac{2C_Y}{a\sigma}\right)_w \sin \beta_w \quad (5)$$

$$\frac{2C_Y}{a\sigma} = -\left(\frac{2C_H}{a\sigma}\right)_w \sin \beta_w + \left(\frac{2C_Y}{a\sigma}\right)_w \cos \beta_w \quad (6)$$

where $(2C_H/a\sigma)_w$ and $(2C_Y/a\sigma)_w$ are in the wind-hub system and are given by

$$\begin{aligned} \left(\frac{2C_H}{a\sigma}\right)_w &= \frac{\delta\mu}{2a} (1 - \epsilon^2) - \frac{1}{4} (\theta_0 - K_1 a_0) \left[2\lambda\mu(1 - \epsilon) - \mu(1 - \epsilon)^2 \frac{\dot{a}_0}{\Omega} \right. \\ &\quad \left. - \left(\epsilon - \frac{2}{3}\right) \left(\frac{\dot{b}_1}{\Omega} - a_1\right) - \frac{2}{3} a_1 + \frac{2}{3} \left(\frac{p}{\Omega} \cos \beta_w + \frac{q}{\Omega} \sin \beta_w\right) \right] \\ &\quad - \frac{\theta_t}{4} \left[\mu\lambda(1 - \epsilon^2) + \frac{\dot{a}_0}{\Omega} \mu \left(\epsilon - \frac{2}{3}\right) - 2 \left(\frac{\epsilon}{3} - \frac{1}{4}\right) \left(\frac{\dot{b}_1}{\Omega} - a_1\right) - \frac{a_1}{2} \right. \\ &\quad \left. + \frac{1}{2} \left(\frac{p}{\Omega} \cos \beta_w + \frac{q}{\Omega} \sin \beta_w\right) \right] + \frac{1}{4} (A_{1c} - K_1 a_1) \left[-\frac{b_1\mu}{4} (1 - \epsilon^2) \right. \\ &\quad \left. + \frac{1}{4} \mu(1 - \epsilon)^2 \left(\frac{\dot{a}_1}{\Omega} + b_1\right) + \frac{2}{3} a_0 + \frac{\mu}{4} (1 - \epsilon^2) \left(-\frac{p}{\Omega} \sin \beta_w + \frac{q}{\Omega} \cos \beta_w\right) \right] \\ &\quad + \frac{1}{4} (B_{1c} - K_1 b_1) \left[\frac{3}{4} \mu(1 - \epsilon)^2 \left(\frac{\dot{b}_1}{\Omega} - a_1\right) + (1 - \epsilon^2) \left(\lambda - \frac{a_1\mu}{4}\right) + \left(\epsilon - \frac{2}{3}\right) \frac{\dot{a}_0}{\Omega} \right. \\ &\quad \left. + \frac{3\mu}{4} (1 - \epsilon^2) \left(\frac{p}{\Omega} \cos \beta_w + \frac{q}{\Omega} \sin \beta_w\right) \right] + \frac{1}{4} \left\{ \epsilon(1 - \epsilon) \left(\frac{\dot{b}_1}{\Omega} - a_1\right) 4\lambda \right. \\ &\quad \left. - (1 - \epsilon^2) \left[2\lambda \left(\frac{\dot{b}_1}{\Omega} - a_1\right) - a_1\lambda \right] - \left(\frac{2}{3} - \epsilon\right) \left[a_1 \frac{\dot{a}_0}{\Omega} + a_0 \left(\frac{\dot{a}_1}{\Omega} + b_1\right) \right] \right. \\ &\quad \left. - \frac{2a_0}{3} \left(-\frac{p}{\Omega} \sin \beta_w + \frac{q}{\Omega} \cos \beta_w\right) - \left[2(1 - \epsilon^2)\lambda - 4 \left(\frac{1}{3} - \frac{\epsilon}{2}\right) \frac{\dot{a}_0}{\Omega} \right] \left(\frac{p}{\Omega} \cos \beta_w \right. \right. \\ &\quad \left. \left. + \frac{q}{\Omega} \sin \beta_w\right) + 4 \frac{a_0}{\Omega} \left(\frac{\dot{b}_1}{\Omega} - a_1\right) \left(\frac{1}{3} - \epsilon + \epsilon^2\right) \right\} + \frac{\mu}{4} \left\{ \epsilon(1 - \epsilon) \left[a_1 \left(\frac{\dot{b}_1}{\Omega} - a_1\right) \right. \right. \\ &\quad \left. \left. + b_1 \left(\frac{\dot{a}_1}{\Omega} + b_1\right) \right] + \frac{1}{4} (1 - \epsilon)^2 \left[b_1 \left(\frac{\dot{a}_1}{\Omega} + b_1\right) + a_1 \left(\frac{\dot{b}_1}{\Omega} - a_1\right) \right] \right\} \quad (7) \end{aligned}$$

(Continued)

$$\begin{aligned}
& - \frac{1}{2} (1 - \epsilon^2) \left[a_1 \left(\frac{\dot{b}_1}{\Omega} - a_1 \right) + b_1 \left(\frac{\dot{a}_1}{\Omega} + b_1 \right) - 2a_0^2 - \frac{b_1^2}{2} - \frac{3}{2} a_1^2 \right] \\
& - \frac{a_1}{4} (1 - \epsilon^2) \left(\frac{p}{\Omega} \cos \beta_w + \frac{q}{\Omega} \sin \beta_w \right) - \frac{b_1}{4} (1 - \epsilon^2) \left(- \frac{p}{\Omega} \sin \beta_w + \frac{q}{\Omega} \cos \beta_w \right) \Big\} \\
& \hspace{15em} (7) \\
& \hspace{15em} \text{(Concluded)}
\end{aligned}$$

and

$$\begin{aligned}
\left(\frac{2C_Y}{a\sigma} \right)_w &= - \frac{1}{4} (\theta_0 - K_1 a_0) \left\{ \left[\left(\epsilon - \frac{2}{3} \right) \left(\frac{\dot{a}_1}{\Omega} + b_1 \right) - \frac{2}{3} b_1 \right] + 3a_0 (1 - \epsilon^2) \mu - 2b_1 (1 - \epsilon) \mu^2 \right. \\
& - \frac{2}{3} \left(- \frac{p}{\Omega} \sin \beta_w + \frac{q}{\Omega} \cos \beta_w \right) \Big\} - \frac{\theta_t}{4} \left\{ \left[\left(\frac{2\epsilon}{3} - \frac{1}{2} \right) \left(\frac{\dot{a}_1}{\Omega} + b_1 \right) - \frac{b_1}{2} \right] \right. \\
& + 2a_0 \mu - b_1 (1 - \epsilon^2) \mu^2 - \frac{1}{2} \left(- \frac{p}{\Omega} \sin \beta_w + \frac{q}{\Omega} \cos \beta_w \right) \Big\} \\
& - \frac{1}{4} (A_{1c} - K_1 a_1) \left\{ \left[\left(\epsilon - \frac{2}{3} \right) \frac{\dot{a}_0}{\Omega} + \lambda (1 - \epsilon^2) \right] + \mu \left[\frac{5a_1}{4} (1 - \epsilon^2) \right. \right. \\
& + \left. \left. \frac{1}{4} (1 - \epsilon)^2 \left(\frac{\dot{b}_1}{\Omega} - a_1 \right) \right] + \frac{\mu}{4} (1 - \epsilon^2) \left(\frac{p}{\Omega} \cos \beta_w + \frac{q}{\Omega} \sin \beta_w \right) \right\} \\
& - \frac{1}{4} (B_{1c} - K_1 b_1) \left\{ - \frac{2}{3} a_0 + \mu \left[\frac{7}{4} b_1 (1 - \epsilon^2) + \frac{1}{4} (1 - \epsilon)^2 \left(\frac{\dot{a}_1}{\Omega} + b_1 \right) \right. \right. \\
& + \left. \left. \frac{1}{4} \left(- \frac{p}{\Omega} \sin \beta_w + \frac{q}{\Omega} \cos \beta_w \right) \right] - \mu^2 [2a_0 (1 - \epsilon)] \right\} \\
& - \frac{1}{4} \left\{ 4 \left(\frac{1}{3} - \epsilon + \epsilon^2 \right) \frac{\dot{a}_0}{\Omega} \left(\frac{\dot{a}_1}{\Omega} + b_1 \right) - 2\lambda (1 - \epsilon)^2 \left(\frac{\dot{a}_1}{\Omega} + b_1 \right) \right. \\
& + \frac{2a_0}{3} \left(\frac{p}{\Omega} \cos \beta_w + \frac{q}{\Omega} \sin \beta_w \right) + 2a_0 \left(\frac{1}{3} - \frac{\epsilon}{2} \right) \left(\frac{\dot{b}_1}{\Omega} - a_1 \right) - 2b_1 \left[\frac{\lambda}{2} (1 - \epsilon^2) \right. \\
& - \left. \left. \frac{\dot{a}_0}{\Omega} \left(\frac{1}{3} - \frac{\epsilon}{2} \right) \right] + \left[4 \left(\frac{1}{3} - \frac{\epsilon}{2} \right) \frac{\dot{a}_0}{\Omega} - 2(1 - \epsilon^2) \lambda \right] \left(- \frac{p}{\Omega} \sin \beta_w + \frac{q}{\Omega} \cos \beta_w \right) \Big\} \\
& - \frac{\mu}{4} \left[6a_0 \lambda (1 - \epsilon) - \frac{a_1 b_1}{2} (1 - \epsilon^2) - 3(1 - \epsilon)^2 a_0 \frac{\dot{a}_0}{\Omega} \right. \\
& - \frac{7}{4} (1 - \epsilon)^2 a_1 \left(\frac{\dot{a}_1}{\Omega} + b_1 \right) + 2b_1 (1 - \epsilon^2) \left(\frac{p}{\Omega} \cos \beta_w + \frac{q}{\Omega} \sin \beta_w \right) \\
& - 2a_1 (1 - \epsilon^2) \left(- \frac{p}{\Omega} \sin \beta_w + \frac{q}{\Omega} \cos \beta_w \right) - \frac{5}{4} (1 - \epsilon)^2 b_1 \left(\frac{\dot{b}_1}{\Omega} - a_1 \right) \Big] \\
& - \mu^2 [a_0 a_1 (1 - \epsilon)] \hspace{15em} (8)
\end{aligned}$$

Main Rotor Hub Moments

The expressions for the main rotor hub moments are:

$$M_{HF} = (M_H)_w \cos \beta_w + (L_H)_w \sin \beta_w \quad (9)$$

$$L_{HF} = -(M_H)_w \sin \beta_w + (L_H)_w \cos \beta_w \quad (10)$$

where

$$\begin{aligned} (M_H)_w = & \frac{N}{2} \left[K_\beta a_1 - \frac{eM_\beta}{g} (\ddot{a}_1 + 2\dot{b}_1\Omega - a_1\Omega^2) \right] - \frac{N}{2} I_\beta \Omega^2 \gamma \epsilon \left\{ -\left[\frac{1}{6} + \frac{\mu^2}{8} (1 - \epsilon) \right] \right. \\ & \times (A_{1c} - K_1 a_1) - \frac{\mu}{4} (1 - \epsilon^2) a_0 + \frac{\mu^2}{8} (1 - \epsilon) b_1 + \left(\frac{1}{6} - \frac{\epsilon}{4} \right) \left(\frac{\dot{a}_1}{\Omega} + b_1 \right) \\ & \left. + \frac{1}{6} \left(-\frac{p}{\Omega} \sin \beta_w + \frac{q}{\Omega} \cos \beta_w \right) \right\} \quad (11) \end{aligned}$$

and

$$\begin{aligned} (L_H)_w = & \frac{N}{2} \left[K_\beta b_1 - \frac{eM_\beta}{g} (\ddot{b}_1 - 2\dot{a}_1\Omega - b_1\Omega^2) \right] - \frac{N}{2} I_\beta \Omega^2 \gamma \epsilon \left\{ \frac{\mu}{2} (1 - \epsilon^2) (\theta_0 - K_1 a_0) \right. \\ & - \left[\frac{1}{6} + \frac{3}{8} \mu^2 (1 - \epsilon) \right] (B_{1c} - K_1 b_1) + \frac{\mu}{3} c_t + \frac{\mu}{2} (1 - \epsilon) \lambda + \frac{\mu^2}{8} (1 - \epsilon) a_1 \\ & \left. - \frac{\mu}{4} (1 - \epsilon)^2 \frac{\dot{a}_0}{\Omega} + \left(\frac{1}{6} - \frac{\epsilon}{4} \right) \left(\frac{\dot{b}_1}{\Omega} - a_1 \right) + \frac{1}{6} \left(\frac{p}{\Omega} \cos \beta_w + \frac{q}{\Omega} \sin \beta_w \right) \right\} \quad (12) \end{aligned}$$

Main Rotor Torque

The expressions for the main rotor torque are:

$$Q_F = \frac{N}{2} \rho a c R^2 (\Omega R)^2 \frac{2C_Q}{a\sigma} \quad (13)$$

$$\begin{aligned} \frac{2C_Q}{a\sigma} = & \frac{\delta}{4a} [1 + (1 - \epsilon^2)\mu^2] - (\theta_0 - K_1 a_0) \left[\frac{\lambda}{3} + \left(\frac{\epsilon}{3} - \frac{1}{4} \right) \frac{\dot{a}_0}{\Omega} + \frac{\mu}{6} \left(\frac{\dot{b}_1}{\Omega} \right) \right. \\ & - \frac{\mu\epsilon}{4} \left(\frac{\dot{b}_1}{\Omega} - a_1 \right) + \frac{\mu}{6} \left(\frac{p}{\Omega} \cos \beta_w + \frac{q}{\Omega} \sin \beta_w \right) \left. \right] - (A_{1c} - K_1 a_1) \left[\left(\frac{1}{8} - \frac{\epsilon}{6} \right) \left(\frac{\dot{a}_1}{\Omega} + b_1 \right) \right. \\ & \left. - \frac{\mu}{6} a_0 + \frac{b_1}{16} (1 - \epsilon^2)\mu^2 + \frac{1}{8} \left(-\frac{p}{\Omega} \sin \beta_w + \frac{q}{\Omega} \cos \beta_w \right) \right] \\ & - (B_{1c} - K_1 b_1) \left[\left(\frac{1}{8} - \frac{\epsilon}{6} \right) \left(\frac{\dot{b}_1}{\Omega} - a_1 \right) + \left(\frac{\epsilon}{4} - \frac{1}{6} \right) \mu \frac{\dot{a}_0}{\Omega} + \frac{1}{2} (1 - \epsilon^2) \left(\frac{\mu\lambda}{2} + \frac{a_1}{8} \mu^2 \right) \right] \quad (14) \end{aligned}$$

(Continued)

$$\begin{aligned}
& + \frac{1}{8} \left(\frac{p}{\Omega} \cos \beta_w + \frac{q}{\Omega} \sin \beta_w \right) \left[- \theta_t \left[\frac{\lambda}{4} + \left(\frac{\epsilon}{4} - \frac{1}{5} \right) \frac{\dot{a}_0}{\Omega} + \frac{\mu}{8} \left(\frac{\dot{b}_1}{\Omega} \right) - \frac{\epsilon \mu}{6} \left(\frac{\dot{b}_1}{\Omega} - a_1 \right) \right] \right. \\
& - \frac{1}{2} (1 - \epsilon^2) \left\{ \lambda^2 + \lambda \mu a_1 + 2 \lambda \epsilon \frac{\dot{a}_0}{\Omega} + \mu \epsilon \left[a_1 \frac{\dot{a}_0}{\Omega} + a_0 \left(\frac{\dot{a}_1}{\Omega} + b_1 \right) \right] \right. \\
& + \mu^2 \left(\frac{a_0^2}{2} + \frac{3}{8} a_1^2 + \frac{1}{8} b_1^2 \right) \left. \right\} + \frac{\mu}{3} \left[a_1 \left(\frac{\dot{a}_0}{\Omega} \right) + a_0 \left(\frac{\dot{a}_1}{\Omega} + b_1 \right) \right] + \frac{2}{3} \lambda \left(\frac{\dot{a}_0}{\Omega} \right) \\
& - \left[- \frac{\mu}{3} a_0 + \left(\frac{1}{4} - \frac{\epsilon}{3} \right) \left(\frac{\dot{a}_1}{\Omega} + b_1 \right) \right] \left(- \frac{p}{\Omega} \sin \beta_w + \frac{q}{\Omega} \cos \beta_w \right) \\
& - \left(\frac{1}{4} - \frac{\epsilon}{3} \right) \left(\frac{\dot{b}_1}{\Omega} - a_1 \right) \left(\frac{p}{\Omega} \cos \beta_w + \frac{q}{\Omega} \sin \beta_w \right) - \frac{1}{8} \left(- \frac{p}{\Omega} \sin \beta_w + \frac{q}{\Omega} \cos \beta_w \right)^2 \\
& - \frac{1}{8} \left(\frac{p}{\Omega} \cos \beta_w + \frac{q}{\Omega} \sin \beta_w \right)^2 - \left(\frac{1}{4} - \frac{2}{3} \epsilon + \frac{\epsilon^2}{2} \right) \left(\frac{\dot{a}_0}{\Omega} \right)^2 \\
& + \frac{1}{2} \left[\left(\frac{\dot{a}_1}{\Omega} + b_1 \right)^2 + \left(\frac{\dot{b}_1}{\Omega} - a_1 \right)^2 \right] \left. \right\} \tag{14}
\end{aligned}$$

(Concluded)

For the case of a two-bladed teetering rotor, the forces and moments may be obtained by setting $\epsilon = 0$, $\dot{a}_0 = \ddot{a}_0 = 0$ in the above equations. For a teetering rotor without cyclic pitch, as is used in many tail rotor systems, the forces and moments may be obtained by setting $A_{1c} = B_{1c} = 0$. Further, since the tail rotor flapping frequency is much higher than that of the main rotor system, the tip-path plane dynamics may be neglected. Thus, for tail rotor applications, one simply sets $\dot{a}_0 = \dot{a}_1 = \dot{b}_1 = 0$, and $\ddot{a}_0 = \ddot{a}_1 = \ddot{b}_1 = 0$ in the above equations. The result is a set of basic quasi-static forces and moment expressions similar to those in the classical work (refs. 9, 10).

These rotor forces and moments, which were then transformed to the center of gravity of the aircraft, represent the contribution of the main rotor to the total aerodynamic forces and moments in the body axes of the aircraft. From figure 3 it can be seen that the transformation is simply:

$$\left. \begin{aligned}
X_F &= T_F \sin i_F - H_F \cos i_F \\
Y_F &= Y_F \\
Z_F &= -T_F \cos i_F - H_F \sin i_F \\
L_F &= L_{HF} \cos i_F - Q_F \sin i_F + Y_F h_F + (T_F \cos i_F + H_F \sin i_F) d_F \\
M_F &= M_{HF} - (T_F \sin i_F - H_F \cos i_F) h_F + (T_F \cos i_F + H_F \sin i_F) \ell_F \\
N_F &= Q_F \cos i_F + L_{HF} \sin i_F + Y_F \ell_F + (T_F \sin i_F - H_F \cos i_F) d_F
\end{aligned} \right\} \tag{15}$$

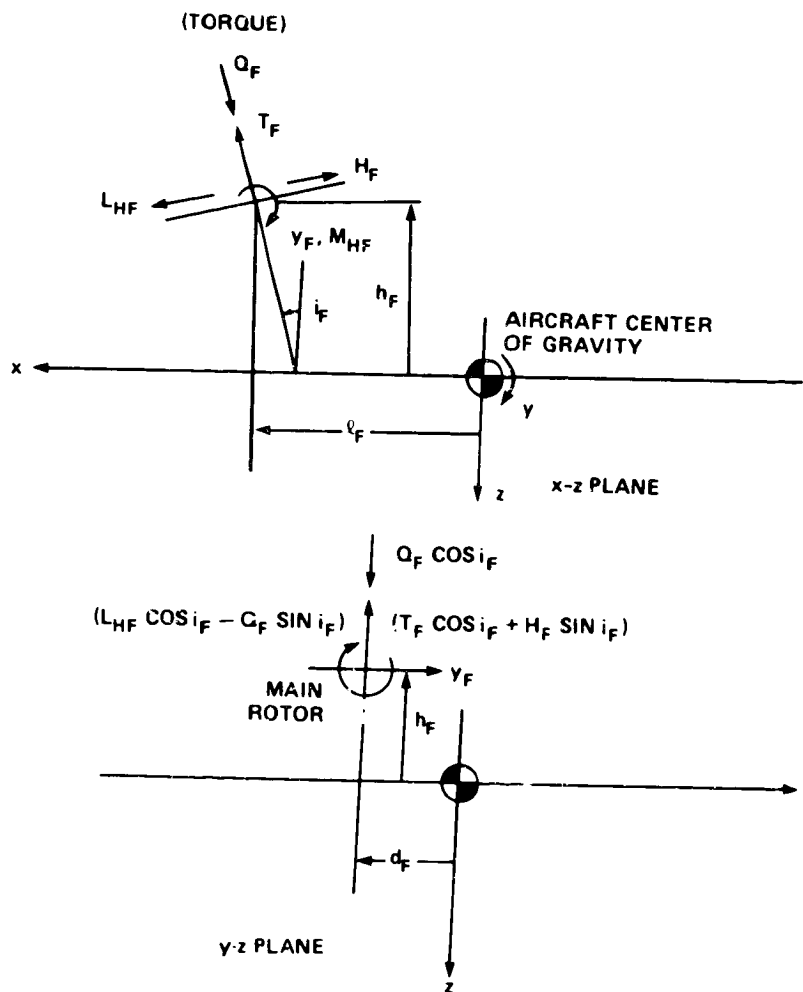


Figure 3.- Main rotor forces and hub moments diagram with respect to aircraft center of gravity.

Table 1 shows the general configuration of the nine-degree-of-freedom (DOF) mathematical model, which consists of three-DOF tip-path plane dynamics and six-DOF rigid-body dynamics. Note that the aerodynamic force terms Δx , ΔY , and ΔZ , and the moment terms ΔL , ΔM , and ΔN are those contributed by the tail rotor, fuselage, horizontal stabilizer and the vertical fin.

CONTROL PHASING

It is evident from equations (A2) that the flapping frequency will generally be different from the rotational frequency of the rotor system. Therefore, the maximum flapping response to a cyclic-control input will no longer exhibit 90° lag in phase. Proper control phasing will be required to achieve the desired flapping decoupling, that is, a longitudinal-control input

TABLE 1.- GENERALIZED SINGLE ROTOR HELICOPTER MATHEMATICAL MODEL
(NINE DEGREES OF FREEDOM, FIRST HARMONIC)

Dynamic equations:

$$\left. \begin{aligned} \dot{V} &= \frac{1}{m} F_G - W_x V + \frac{1}{m} F_A(V, \omega; \underline{a}, \dot{\underline{a}}; \underline{u}) \\ \dot{\omega} &= -I^{-1} W_x I \omega + I^{-1} M_A(V, \omega; \underline{a}, \dot{\underline{a}}; \underline{u}) \end{aligned} \right\} \begin{array}{l} \text{Euler} \\ \text{equations} \end{array}$$

$$\frac{d}{dt} \begin{pmatrix} \underline{a} \\ \dot{\underline{a}} \end{pmatrix} = \begin{pmatrix} 0_3 & I_3 \\ -\tilde{K} & -\tilde{D} \end{pmatrix} \begin{pmatrix} \underline{a} \\ \dot{\underline{a}} \end{pmatrix} + \begin{bmatrix} 0 \\ \tilde{f}(V, \omega; \underline{a}, \dot{\underline{a}}; \underline{u}) \end{bmatrix} \quad \begin{array}{l} \text{Tip-path-} \\ \text{plane} \\ \text{equations} \end{array}$$

Kinematic equations:

$$V_e = [L_{B-E}]^T V$$

$$\frac{d}{dt} \begin{pmatrix} \theta \\ \phi \\ \psi \end{pmatrix} = \begin{pmatrix} 0 & \cos \phi & -\sin \phi \\ 1 & \sin \phi \tan \theta & \cos \phi \tan \theta \\ 0 & \sin \phi \sec \theta & \cos \phi \sec \theta \end{pmatrix} \omega$$

where

$$V = (u, v, w)^T; \quad \omega = (p, q, r)^T; \quad \underline{a} = (a_0, a_1, b_1)^T$$

$$V_e = (\dot{x}_e, \dot{y}_e, -\dot{h})^T$$

$$F_G = mg(-\sin \theta, \sin \phi \cos \theta, \cos \phi \cos \theta)^T; \quad \underline{u} = (A_{1c}, B_{1c}, \theta_0, \theta_{0t})^T$$

$$F_A = (X, Y, Z)^T = (X_F + \Delta X, Y_F + \Delta Y, Z_F + \Delta Z)^T$$

$$M_A = (L, M, N)^T = (L_F + \Delta L, M_F + \Delta M, N_F + \Delta N)^T$$

$$I = \begin{bmatrix} I_x & 0 & -I_{xz} \\ 0 & I_y & 0 \\ -I_{xz} & 0 & I_z \end{bmatrix} \quad W_x = \begin{bmatrix} 0 & -r & q \\ r & 0 & -p \\ -q & p & 0 \end{bmatrix}$$

$$L_{B-E} = \begin{bmatrix} \cos \theta \cos \psi & \cos \theta \sin \psi & -\sin \theta \\ \sin \theta \sin \phi \sin \psi - \cos \phi \sin \psi & \sin \theta \sin \phi \sin \psi + \cos \phi \sin \psi & \sin \phi \cos \theta \\ \sin \theta \cos \phi \cos \psi + \sin \phi \sin \psi & \sin \theta \cos \phi \sin \psi - \sin \phi \cos \psi & \cos \phi \cos \theta \end{bmatrix}$$

produces only a steady-state longitudinal flapping, and a lateral-control input will produce only the lateral flapping response. A detailed discussion on the question of control phasing (or control mixing) is given in reference 8.

A set of simplified equations based on hovering flight has been developed to achieve the desired flapping-response decoupling. The equations relate the required control phasing to the rotor system parameters, that is,

$$\begin{pmatrix} A_{1s} \\ B_{1s} \end{pmatrix} = \begin{pmatrix} \frac{\partial A_{1s}}{\partial \delta A} & \frac{\partial A_{1s}}{\partial \delta L} \\ \frac{\partial B_{1s}}{\partial \delta A} & \frac{\partial B_{1s}}{\partial \delta L} \end{pmatrix} \begin{pmatrix} \delta_A \\ \delta_L \end{pmatrix} \quad (16)$$

$$\left. \begin{aligned} \frac{\partial A_{1s}}{\partial \delta A} &= \frac{1 - (8/3)\epsilon + 2\epsilon^2}{1 - (4/3)\epsilon} k_2 \\ \frac{\partial B_{1s}}{\partial \delta A} &= \frac{8(P^2 - 1)}{\gamma[1 - (4/3)\epsilon]} k_2 \\ \frac{\partial A_{1s}}{\partial \delta L} &= \frac{8(P^2 - 1)}{\gamma[1 - (4/3)\epsilon]} k_1 \\ \frac{\partial B_{1s}}{\partial \delta L} &= \frac{-[1 - (8/3)\epsilon + 2\epsilon^2]}{1 - (4/3)\epsilon} K_1 \end{aligned} \right\} \quad (17)$$

with

$$P^2 - 1 = \frac{K_\beta}{I_\beta \Omega^2} + \frac{eM_\beta}{I_\beta} + \frac{\gamma K_1}{8} \left(1 - \frac{4}{3} \epsilon\right)$$

The so-called control advance angle ϕ is given by

$$\begin{aligned} \tan \phi &= \frac{\partial B_{1s} / \partial \delta A}{\partial A_{1s} / \partial \delta A} \\ &= \frac{P^2 - 1}{\gamma(1/8 - \epsilon/3 + \epsilon^2/4)} \end{aligned} \quad (18)$$

The control crossfeed given by equation (17) has provided an accuracy adequate for the entire low-speed flight regime.

CONCLUDING REMARKS

A simplified nine-degree-of-freedom, main rotor, mathematical model has been developed for real-time, piloted simulation for exploratory investigations of helicopter flying qualities. The model explicitly contains the dynamic effects of the tip-path plane and several primary design parameters of interest, such as flapping hinge restraint, effective hinge offset, blade Lock number, and pitch-flap coupling. Furthermore, being analytical, the model provides insight useful for designing simulation experiments.

It should be emphasized, however, that the simplified mathematical model is suitable only for stability and control applications. Because of the basic assumptions used in its development, applications of the model should be limited to an advance ratio of about 0.3. Beyond that, the model must be modified to account for the stall and compressibility effects. Incorporating the rotor rotational degree of freedom, ground and turbulence effects, and inflow dynamics would enhance the model's validity for a wider range of applications.

APPENDIX A

Flapping Equation of Motion

Given the basic assumptions noted in the text, the flapping equations of motion have been developed in reference 8 for a rotor system containing design parameters, such as flapping hinge restraint, hinge offset, and pitch-flap coupling. For convenience, they are given here for both two-bladed teetering rotors and nonteetering rotors.

Two-Bladed Teetering Rotor

$$\begin{aligned}
 \ddot{\beta} + \frac{\Omega Y}{8} \dot{\beta} + \Omega^2 \left[P^2 + \frac{\gamma \mu^2}{8} \sin 2\psi + \frac{\gamma K_1 \mu^2}{8} (1 - \cos 2\psi) \right] \beta \\
 = \Omega^2 \left\{ \left[2 \left(\frac{P}{\Omega} \sin \beta_w - \frac{q}{\Omega} \cos \beta_w \right) + \left(\frac{\dot{P}}{\Omega^2} \cos \beta_w + \frac{\dot{q}}{\Omega^2} \sin \beta_w \right) + \frac{\gamma}{8} \left(\frac{P}{\Omega} \cos \beta_w \right. \right. \right. \\
 \left. \left. + \frac{q}{\Omega} \sin \beta_w \right) \right] \sin \psi + \left[2 \left(\frac{P}{\Omega} \cos \beta_w + \frac{q}{\Omega} \sin \beta_w \right) - \left(\frac{\dot{P}}{\Omega^2} \sin \beta_w - \frac{\dot{q}}{\Omega^2} \cos \beta_w \right) \right. \\
 \left. - \frac{\gamma}{8} \left(\frac{P}{\Omega} \sin \beta_w - \frac{q}{\Omega} \cos \beta_w \right) \right] \cos \psi + \left(\frac{\gamma \mu}{3} \sin \psi \right) \theta_0 - \frac{\gamma}{8} \left[\left(1 + \frac{1}{2} \mu^2 \right) \cos \psi \right. \\
 \left. - \frac{\mu^2}{2} \cos 3\psi \right] A_{1c} - \frac{\gamma}{8} \left[\left(1 + \frac{3}{2} \mu^2 \right) \sin \psi - \frac{\mu^2}{2} \sin 3\psi \right] B_{1c} \\
 \left. + \frac{\gamma \mu}{4} (\sin \psi) \theta_t + \frac{\gamma \mu}{4} (\sin \psi) \lambda \right\} \quad (A1)
 \end{aligned}$$

where

$$P^2 = 1 + \frac{K_\beta}{I_\beta \Omega^2} + \frac{K_1 \gamma}{8}$$

N-Bladed Nonteetering Rotor

$$\begin{aligned}
 \ddot{\beta}_i + \frac{\gamma \Omega}{2} \left[\left(\frac{1}{4} - \frac{2}{3} \epsilon + \frac{\epsilon^2}{2} \right) + \mu \left(\frac{1}{3} - \epsilon + \epsilon^2 \right) \sin \psi_i \right] \dot{\beta}_i \\
 + \Omega^2 \left\{ P^2 + \frac{\gamma}{2} \left[\mu \left(\frac{1}{3} - \frac{\epsilon}{2} \right) \cos \psi_i + \frac{\mu^2}{2} \left(\frac{1}{2} - \epsilon + \frac{\epsilon^2}{2} \right) \sin 2\psi_i \right] \right. \\
 \left. + \frac{\gamma K_1}{2} \left[\mu \left(\frac{2}{3} - \epsilon \right) \sin \psi_i + \frac{\mu^2}{2} \left(\frac{1}{2} - \epsilon + \frac{\epsilon^2}{2} \right) (1 - \cos 2\psi_i) \right] \right\} \beta_i \\
 = \Omega^2 \left\{ 2 \left(1 + \frac{e M_\beta}{I_\beta} \right) \left[\left(\frac{P}{\Omega} \sin \beta_w - \frac{q}{\Omega} \cos \beta_w \right) \sin \psi_i + \left(\frac{P}{\Omega} \cos \beta_w + \frac{q}{\Omega} \sin \beta_w \right) \cos \psi_i \right] \right\} \quad (A2)
 \end{aligned}$$

(Continued)

$$\begin{aligned}
& + \left(\frac{\dot{p}}{\Omega^2} \cos \beta_w + \frac{\dot{q}}{\Omega^2} \sin \beta_w \right) \sin \psi_i - \left(\frac{\dot{p}}{\Omega^2} \sin \beta_w - \frac{\dot{q}}{\Omega^2} \cos \beta_w \right) \cos \psi_i \\
& + \frac{M_\beta}{I_\beta \Omega^2} [(\dot{w} - uq + pv) - g] + \frac{\gamma}{2} \left[\left(\frac{1}{4} - \frac{\epsilon}{3} \right) + \left(\frac{2}{3} - \epsilon \right) \mu \sin \psi_i \right. \\
& + \left. \frac{\mu^2}{2} \left(\frac{1}{2} - \epsilon + \frac{\epsilon^2}{2} \right) (1 - \cos 2\psi_i) \right] \theta_o - \frac{\gamma}{2} \left[\left(\frac{1}{4} - \frac{\epsilon}{3} \right) \cos \psi_i + \mu \left(\frac{1}{3} - \frac{\epsilon}{2} \right) \sin 2\psi_i \right. \\
& + \left. \frac{\mu^2}{4} \left(\frac{1}{2} - \epsilon + \frac{\epsilon^2}{2} \right) (\cos \psi_i - \cos 3\psi_i) \right] A_{1c} - \frac{\gamma}{2} \left[\left(\frac{1}{4} - \frac{\epsilon}{3} \right) \sin \psi_i \right. \\
& + \left. \mu \left(\frac{1}{3} - \frac{\epsilon}{2} \right) (1 - \cos 2\psi_i) + \frac{\mu^2}{4} \left(\frac{1}{2} - \epsilon + \frac{\epsilon^2}{2} \right) (3 \sin \psi_i - \sin 3\psi_i) \right] B_{1c} \\
& + \frac{\gamma}{2} \left[\left(\frac{1}{5} - \frac{\epsilon}{4} \right) + \mu \left(\frac{1}{2} - \frac{2}{3} \epsilon \right) \sin \psi_i + \frac{\mu^2}{2} \left(\frac{1}{3} - \frac{\epsilon}{2} \right) (1 - \cos 2\psi_i) \right] \theta_t \\
& + \frac{\gamma}{2} \left[\left(\frac{1}{3} - \frac{\epsilon}{2} \right) + \mu \left(\frac{1}{2} - \epsilon + \frac{\epsilon^2}{2} \right) \sin \psi_i \right] \lambda \left\{ + \frac{\gamma}{2} \left(\frac{1}{4} - \frac{\epsilon}{3} \right) \left[\left(\frac{p}{\Omega} \cos \beta_w \right. \right. \right. \\
& + \left. \left. \frac{q}{\Omega} \sin \beta_w \right) \sin \psi_i - \left(\frac{p}{\Omega} \sin \beta_w - \frac{q}{\Omega} \cos \beta_w \right) \cos \psi_i \right] \\
& + \frac{\gamma}{8} \mu \left(\frac{2}{3} - \epsilon \right) \left[\left(\frac{p}{\Omega} \cos \beta_w + \frac{q}{\Omega} \sin \beta_w \right) (1 - \cos 2\psi_i) - \left(\frac{p}{\Omega} \sin \beta_w \right. \right. \\
& \left. \left. - \frac{q}{\Omega} \cos \beta_w \right) \sin 2\psi_i \right]
\end{aligned} \tag{A2}$$

(Concluded)

where

$$p^2 = 1 + \frac{eM_\beta}{I_\beta} + \frac{K_\beta}{I_\beta \Omega^2} + \frac{\gamma K_1}{8} \left(1 - \frac{4}{3} \epsilon \right)$$

$$i = 1, 2, 3, \dots, N$$

APPENDIX B

Derivation of Rotor Force and Moment Expressions

The derivations of the rotor forces and moments will be performed first in the wind-hub system (see fig. 2). Then, they will be transformed into the hub-body system to be added to the other components contributing to the total aircraft forces and moments. Only the development of thrust is given here to illustrate the procedure. The development of other forces and moments is given in a forthcoming report.²

The shear force for a single i th blade at azimuth ψ_i is given by

$$\begin{aligned}
 S(\psi_i) = & F_a - \ddot{\beta} M_\beta - m\dot{q} + m(\dot{w} - u\dot{q} + p\dot{v}) \\
 & + \left[2p\Omega \left(\frac{M_\beta}{g} + em \right) + \frac{M_\beta}{g} \dot{q} \right] \cos \psi_i' \\
 & + \left[-2q\Omega \left(\frac{M_\beta}{g} + em \right) + \frac{M_\beta}{g} \dot{p} \right] \sin \psi_i'
 \end{aligned} \tag{B1}$$

where the aerodynamic force acting on the blade is again given by

$$F_a = \int_0^{R-e} \frac{\rho}{2} (\Omega R)^2 ac (\bar{U}_T^2 \theta + \bar{U}_T \bar{U}_P) dr' \tag{B2}$$

Substituting the following equations,

$$\bar{U}_T = \frac{U_T}{\Omega R} = \epsilon (1 - \cos \beta) + \mu \sin \psi + x \cos \beta \tag{B3a}$$

$$\begin{aligned}
 \bar{U}_P = \frac{U_P}{\Omega R} = & \lambda \cos \beta - \mu \sin \beta \cos \psi - \frac{\dot{\beta}}{\Omega} (x - \epsilon) \\
 & + x \left[\left(\frac{p}{\Omega} \cos \beta_w + \frac{q}{\Omega} \sin \beta_w \right) \sin \psi + \left(-\frac{p}{\Omega} \sin \beta_w + \frac{q}{\Omega} \cos \beta_w \right) \cos \psi \right]
 \end{aligned} \tag{B3b}$$

$$\theta = \theta_0 - A_{1c} \cos \psi - B_{1c} \sin \psi + x\theta_t - K_1 \beta \tag{B3c}$$

into equation (B2) results in F_a becoming

²Chen, R. T. N.; and Decker, W. A.: Effects of Primary Rotor Parameters on Helicopter Stability and Control Characteristics (in preparation).

$$\begin{aligned}
F_a = \frac{\rho}{2} (\Omega R)^2 acR & \left\{ \left[\frac{1}{3} + (1 - \epsilon)(1 + \epsilon + \mu \sin \psi) \mu \sin \psi \right] (\theta_0 - A_{1c} \cos \psi - B_{1c} \sin \psi) \right. \\
& + \left[\frac{1}{4} + \left(\frac{2}{3} + \frac{1}{2} \overline{1 - \epsilon^2} \mu \sin \psi \right) \mu \sin \psi \right] \theta_t + \left[\frac{1}{2} (1 - \epsilon^2) + (1 - \epsilon) \mu \sin \psi \right] \lambda \\
& - \left\{ \left[\frac{1}{3} + (1 - \epsilon)(1 + \epsilon + \mu \sin \psi) \mu \sin \psi \right] K_1 + \left[\frac{1}{2} (1 - \epsilon^2) \right. \right. \\
& + \left. \left. (1 - \epsilon) \mu \sin \psi \right] \mu \cos \psi \right\} \beta - \frac{1}{\Omega} \left[\frac{1}{3} - \frac{\epsilon}{2} + \frac{\mu}{2} (1 - \epsilon)^2 \sin \psi \right] \dot{\beta} \\
& + \left[\frac{1}{3} + \frac{\mu}{2} (1 - \epsilon^2) \sin \psi \right] \left[\left(\frac{p}{\Omega} \cos \beta_w + \frac{q}{\Omega} \sin \beta_w \right) \sin \psi \right. \\
& \left. + \left(-\frac{p}{\Omega} \sin \beta_w + \frac{q}{\Omega} \cos \beta_w \right) \cos \psi \right] \left. \right\} \quad (B4)
\end{aligned}$$

The flapping will be approximated by its tip-path plane representation:

$$\beta = a_0(t) - a_1(t) \cos \psi - b_1(t) \sin \psi \quad (B5a)$$

thus,

$$\dot{\beta} = \dot{a}_0 - (\dot{a}_1 + b_1 \Omega) \cos \psi - (\dot{b}_1 - a_1 \Omega) \sin \psi \quad (B5b)$$

$$\ddot{\beta} = \ddot{a}_0 - (\ddot{a}_1 + 2\dot{b}_1 \Omega - a_1 \Omega^2) \cos \psi - (\ddot{b}_1 - 2\dot{a}_1 \Omega - b_1 \Omega^2) \sin \psi \quad (B5c)$$

Noting that

$$\sum_{i=1}^N \sin \psi_i = \sum_{i=1}^N \sin \psi'_i = 0$$

$$\sum_{i=1}^N \cos \psi_i = \sum_{i=1}^N \cos \psi'_i = 0$$

the thrust becomes

$$T = \sum_{i=1}^N F_a(\psi_i) - N[\ddot{a}_0 M_\beta + mg - m(\dot{w} - uq + pv)] \quad (B6)$$

The first term on the right-hand side of equation (B6) is a function of the number of blades. For example, for $N = 3$ and 4 , the following expression was obtained:

$$\begin{aligned}
\frac{1}{(1/2)\rho acR(\Omega R)^2} \sum_{i=1}^N F_a(\psi_i) = & N \left[\frac{\theta_0}{3} + \frac{\theta_t}{4} + \frac{1}{2} (1 - \epsilon^2)\lambda - \frac{K_1 a_0}{3} - \frac{\dot{a}_0}{\Omega} \left(\frac{1}{3} - \frac{\epsilon}{2} \right) \right] \\
& + \frac{N}{2} \left\{ \mu^2 (1 - \epsilon)\theta_0 + \frac{\mu^2}{2} (1 - \epsilon^2)\theta_t - \mu(1 - \epsilon^2)B_{1c} \right. \\
& - [a_0 \mu^2 (1 - \epsilon) - b_1 \mu (1 - \epsilon^2)]K_1 + \frac{a_1}{2} \mu (1 - \epsilon^2) \\
& + \frac{1}{\Omega} (\dot{b}_1 - a_1 \Omega) \frac{\mu}{2} (1 - \epsilon)^2 \\
& \left. + \frac{\mu}{2} (1 - \epsilon^2) \left(\frac{p}{\Omega} \cos \beta_w + \frac{q}{\Omega} \sin \beta_w \right) \right\} + O(N) \quad (B7)
\end{aligned}$$

where

$$O(4) = 0 \quad (\text{for four-bladed rotor})$$

$$\begin{aligned}
O(3) = & \frac{3}{4} [\mu^2 (1 - \epsilon)B_{1c} - b_1 \mu^2 (1 - \epsilon)K_1 + a_1 \mu^2 (1 - \epsilon)] \sin 3\psi \\
& + \frac{3}{4} [\mu^2 (1 - \epsilon)A_{1c} - (a_1 K_1 + b_1) \mu^2 (1 - \epsilon)] \cos 3\psi
\end{aligned}$$

(for three-bladed rotor)

Finally, the thrust may be expressed as

$$\begin{aligned}
T = & \frac{N}{2} \rho acR(\Omega R)^2 \left\{ \frac{1}{2} (1 - \epsilon^2)\lambda + \left[\frac{1}{3} + \frac{\mu^2}{2} (1 - \epsilon) \right] \theta_0 + \left[\frac{1}{4} + \frac{\mu^2}{4} (1 - \epsilon^2) \right] \theta_t \right. \\
& - \frac{\mu}{2} (1 - \epsilon^2)B_{1c} - a_0 \left[\frac{1}{3} + \frac{\mu^2}{2} (1 - \epsilon) \right] K_1 + a_1 \left[\frac{\mu}{2} \epsilon (1 - \epsilon) \right] \\
& + b_1 \left[\frac{\mu}{2} (1 - \epsilon^2)K_1 \right] - \frac{\dot{a}_0}{\Omega} \left(\frac{1}{3} - \frac{\epsilon}{2} \right) + \frac{\dot{b}_1}{\Omega} \left[\frac{\mu}{4} (1 - \epsilon)^2 \right] \\
& \left. + \frac{\mu}{4} (1 - \epsilon^2) \left(\frac{p}{\Omega} \cos \beta_w + \frac{q}{\Omega} \sin \beta_w \right) + \frac{O(N)}{N} \right\} - N[\ddot{a}_0 M_B + mg - m(\dot{w} - uq + pv)]
\end{aligned}$$

where

$$\begin{aligned}
O(4) = 0 & \quad (\text{for } N = 4) \\
O(3) = & \frac{3}{4} [\mu^2 (1 - \epsilon)B_{1c} - b_1 \mu^2 (1 - \epsilon)K_1 + a_1 \mu^2 (1 - \epsilon)] \sin 3\psi \\
& + \frac{3}{4} [\mu^2 (1 - \epsilon)A_{1c} - \mu^2 (1 - \epsilon)(a_1 K_1 + b_1)] \cos 3\psi \\
& \quad (\text{for } N = 3)
\end{aligned} \quad (B8)$$

By dropping the high harmonic contributions, the thrust can now be expressed as

$$\begin{aligned}
 T = \frac{N}{2} \rho a c R (\Omega R)^2 & \left\{ \frac{1}{2} (1 - \epsilon^2) \lambda + \left[\frac{1}{3} + \frac{\mu^2}{2} (1 - \epsilon) \right] \theta_0 + \left[\frac{1}{4} + \frac{\mu^2}{4} (1 - \epsilon^2) \right] \theta_t \right. \\
 & - \frac{\mu}{2} (1 - \epsilon^2) (B_{1c} - K_1 b_1) - a_0 \left[\frac{1}{3} + \frac{\mu^2}{2} (1 - \epsilon) \right] K_1 + a_1 \left[\frac{\mu}{2} \epsilon (1 - \epsilon) \right] \\
 & - \frac{\dot{a}_0}{\Omega} \left(\frac{1}{3} - \frac{\epsilon}{2} \right) + \frac{\dot{b}_1}{\Omega} \left[\frac{\mu}{4} (1 - \epsilon)^2 \right] + \frac{\mu}{4} (1 - \epsilon^2) \left(\frac{p}{\Omega} \cos \beta_w + \frac{q}{\Omega} \sin \beta_w \right) \left. \right\} \\
 & - N[\ddot{a}_0 M_\beta + mg - m(\dot{w} - uq + pv)] \tag{B9}
 \end{aligned}$$

Because the last two terms, $mg - m(\dot{w} - uq + pv)$, are generally small compared to other terms, they are dropped, as was shown earlier in equation (2).

REFERENCES

1. Davis, J. M.; Bennett, R. L.; and Blankenship, B. L.: Rotorcraft Flight Simulation with Aeroelastic Rotor and Improved Aerodynamic Representation. USAAMRDL-TR-74-10B, June 1974.
2. Anderson, W. D.; Conner, F.; Kretsinger, P.; and Reaser, J. S.: Rexor Rotorcraft Simulation Model. USAAMRDL-TR-76-28A, June 1976.
3. Blake, B. B.; Albion, N.; and Radford, R.: Flight Simulation of the CH46 Helicopter. Paper presented at the 25th American Helicopter Society National Forum, May 1969.
4. Wilcook, T.: RAE Experience in the Use of a Piloted Ground-Based Simulator for Helicopter Handling Studies. AGARD CP-121, Feb. 1973.
5. Chen, R. T. N.; and Talbot, P. D.: An Exploratory Investigation of the Effects of Large Variations in Rotor System Dynamics Design Parameters on Helicopter Handling Characteristics in Nap-of-the-Earth Flight. Paper presented at the 33rd American Helicopter Society National Forum, May 1977.
6. Chen, R. T. N.; Talbot, P. D.; Gerdes, R. M.; and Dugan, D. C.: A Piloted Simulator Investigation on Augmentation Systems to Improve Helicopter Nap-of-the-Earth Handling Qualities. Paper presented at the 34th American Helicopter Society National Forum, May 1978.
7. Forest, R. D.; Chen, R. T. N.; Gerdes, R. M.; Alderete, T. C.; and Gee, D. R.: A Piloted Simulator Investigation of Helicopter Control Systems Effects on Handling Qualities During Instrument Flight. Paper to be presented at 35th American Helicopter Society National Forum, May 1979.
8. Chen, R. T. N.: Effects of Primary Rotor Parameters on Flapping Dynamics. NASA TP-1431, 1979.
9. Gessow, A.; and Myers, G. C., Jr.: Aerodynamics of the Helicopter. Frederick Ungar Pub. Co., New York, 1952.
10. Seckel, E.; and Curtiss, H. C., Jr.: Aerodynamic Characteristics of Helicopter Rotors. Department of Aerospace and Mechanical Engineering Report No. 659, Princeton University, Princeton, New Jersey, 1962.
11. Hohenemser, K. H.; and Yin, S. K.: Some Applications of the Method of Multiblade Coordinates. J. American Helicopter Soc., July 1972, pp. 3-12.

1. Report No. NASA TM-78575	2. Government Accession No.	3. Recipient's Catalog No.	
4. Title and Subtitle A SIMPLIFIED ROTOR SYSTEM MATHEMATICAL MODEL FOR PILOTED FLIGHT DYNAMICS SIMULATION		5. Report Date	
		6. Performing Organization Code	
7. Author(s) Robert T. N. Chen		8. Performing Organization Report No. A-7538	
		10. Work Unit No. 505-10-23	
9. Performing Organization Name and Address Ames Research Center, NASA Moffett Field, Calif. 94035		11. Contract or Grant No.	
		13. Type of Report and Period Covered Technical Memorandum	
12. Sponsoring Agency Name and Address National Aeronautics and Space Administration Washington, D. C. 20546		14. Sponsoring Agency Code	
		15. Supplementary Notes	
16. Abstract <p>This report documents a simplified analytical mathematical model of the helicopter main rotor; the model was developed primarily for real-time pilot-in-the-loop investigation of helicopter flying qualities. The mathematical model explicitly includes the tip-path plane dynamics and several primary rotor design parameters, such as flapping hinge restraint, flapping hinge offset, blade lock number, and pitch-flap coupling. The model has been used in several exploratory studies, recently performed at Ames Research Center, of the flying qualities of helicopters with a variety of rotor systems.</p> <p>The report describes the basic assumptions used and the major steps involved in the development of the set of equations listed. The equations consist of the tip-path plane dynamic equation, the equations for the main rotor forces and moments, and the equation for control phasing required to achieve decoupling in pitch and roll due to cyclic inputs.</p>			
17. Key Words (Suggested by Author(s)) Mathematical model Helicopter rotor system Piloted simulation Stability and control		18. Distribution Statement Unlimited STAR Category - 08	
19. Security Classif. (of this report) Unclassified	20. Security Classif. (of this page) Unclassified	21. No. of Page 27	Price \$4.00

**END
DATE
FILMED**

JUL 31 1979